Large-scale modeling of primary production and ice algal biomass within arctic sea ice in 1992

Clara Deal,[1] Meibing Jin,[1] Scott Elliott,[2] Elizabeth Hunke,[2] Mathew Maltrud,[2] and Nicole Jeffery[2]

Received 18 May 2010; revised 15 February 2011; accepted 22 March 2011; published 8 July 2011.

[1] An ice ecosystem model was coupled to a global dynamic sea ice model to assess large-scale variability of primary production and ice algal biomass within arctic sea ice. The component models are the Physical Ecosystem Model (PhEcoM) ice ecosystem model and the Los Alamos Sea Ice Model (CICE). Simulated annual arctic sea ice primary production was 15.1 Tg C; within the range of 9 to 73 Tg C estimated using in situ data. The amount of C fixed was >3 Tg C month^{-1} for March, April, and May. The Bering Sea, Arctic Ocean basins, and the Canadian Archipelago/Baffin Bay were the most productive regions on an annual basis, contributing approximately 24, 18, and another 18%, respectively. High production in the Bering Sea was due to high daily production rates, while the large sea ice coverage in the Canadian Archipelago/Baffin Bay and, in particular, the Arctic Ocean basins resulted in their considerable contribution to sea ice primary production. The simulated trends, patterns, and seasonality of ice algae agree reasonably well with very limited observations. In the model, ice growth rate controls the availability of nutrients to sea ice algae, such that ocean nutrient supply is of secondary importance to ice algal growth. The numerical model results suggest that ice melt rate, which determines the proportional rate of ice algal release, controls the termination of the bloom on large scales. The model described advances the role of sea ice algae in biogeochemical cycling within global climate models.

Citation: Deal, C., M. Jin, S. Elliott, E. Hunke, M. Maltrud, and N. Jeffery (2011), Large-scale modeling of primary production and ice algal biomass within arctic sea ice in 1992, *J. Geophys. Res.*, *116*, C07004, doi:10.1029/2010JC006409.

1. Introduction

[2] Algae growing within sea ice form a significant portion of the primary production in ice-covered seas. On average, 4% of the Earth's surface is covered by sea ice, but its extent and thickness are rapidly decreasing, and the ice-free season is lengthening because of warming of the Arctic [*Stroeve et al.*, 2007]. The impacts of diminishing arctic sea ice on the marine ecosystem extend well beyond loss of substrate and changes in habitat for sea ice algae. These carbon fixers are the base of the ice-associated food web. They are also an important food source for pelagic and benthic herbivores, and regulators of other biogeochemical processes [*Gosselin et al.*, 1997; *Caroll and Caroll*, 2003]. During the ice melt season, ice algae are released into the water column with the potential to seed the phytoplankton bloom [*Gradinger*, 2009; *Jin et al.*, 2006], extend the growing season, and shape the structure and function of the polar marine food web. An evaluation of the temporal and spatial distribution of sea ice algal primary productivity and biomass on regional scales is crucial for determining their contribution to the carbon cycle of the Arctic Ocean, interactions with other biogeochemical cycles, and importance in providing nutrition for upper trophic levels.

[3] Because of the challenges in making measurements in the ice environment (e.g., logistical, methodological), accessing remote regions, and remotely sensing under ice biology on regional scales, observations of sea ice algae are sparse. Data gaps are particularly apparent for the time period directly preceding and during ice breakup, when logistical constraints severely limit access and sampling operations. On the basis of the information available, >50% of primary production in the central Arctic Ocean is attributed to ice algae [*Gosselin et al.*, 1997]. For arctic shelf seas, the percentage of marine primary production by ice algae is 4–25%, depending upon location [*Legendre et al.*, 1992].

[4] For a few locations where sea ice algal dynamics and habitats have been rather well characterized, ice algal production has been simulated in one dimension [*Lavoie et al.*, 2005], sometimes coupled to biological production models in the water column [*Jin et al.*, 2006, 2007; *Nishi and Tabeta*, 2005], and in two instances, using a sea ice dynamics model [*Lavoie et al.*, 2009, 2010]. These studies have focused on the

[1]International Arctic Research Center, University of Alaska Fairbanks, Fairbanks, Alaska, USA.
[2]Coupled Ocean Sea Ice Modeling, Los Alamos National Laboratory, Los Alamos, New Mexico, USA.

Copyright 2011 by the American Geophysical Union.
0148-0227/11/2010JC006409

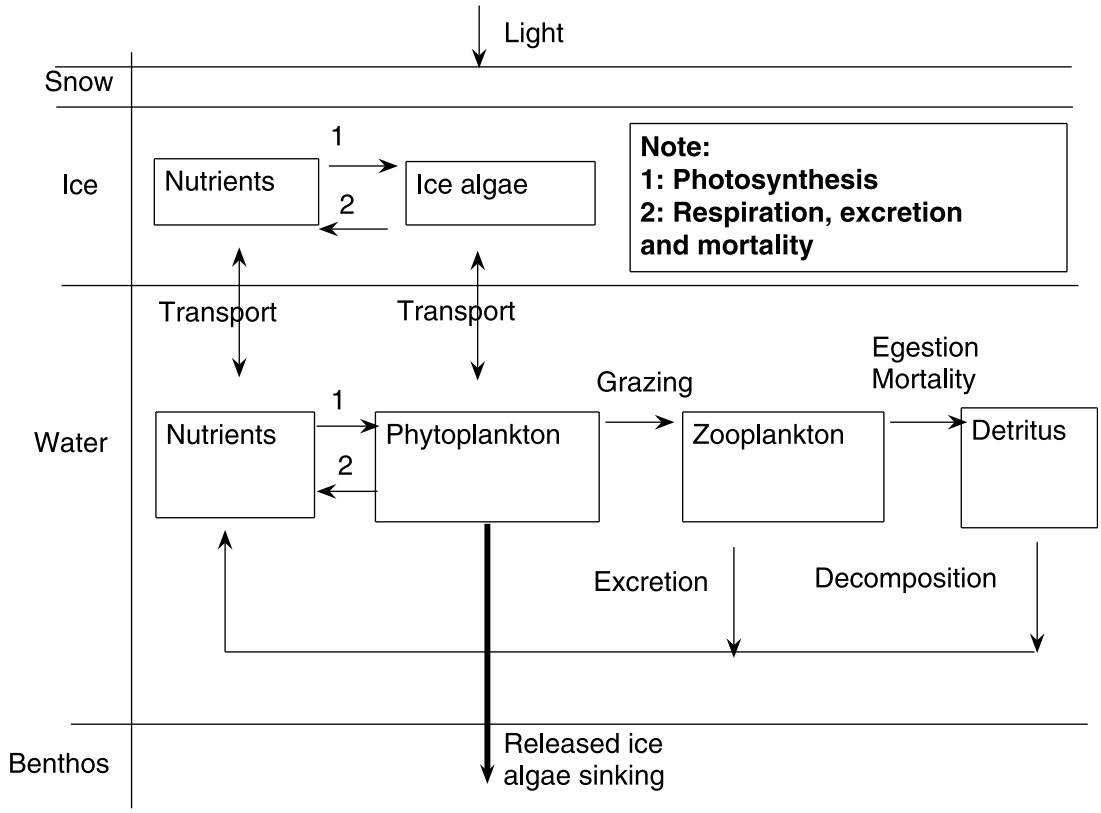

Figure 1. One-dimensional Physical Ecosystem Model (PhEcoM) ice-ocean ecosystem model schematic from *Jin et al.* [2006]. The PhEcoM ice ecosystem model component was coupled to the Los Alamos Sea Ice Model (CICE) in this study.

bottom ice algal community and have thus provided useful information on the local environmental controls and variability of sea ice primary production and biomass. As a first attempt on the regional scale, *Sibert et al.* [2010] have estimated ice algal production using a 3-D ice-ocean model of the Hudson Bay system.

[5] Water-ice transport flux, nutrient supplies, and light availability are important factors on small scales [*Jin et al.*, 2006; *Lavoie et al.*, 2005]. Observations show that regional differences in sea ice primary production are largely driven by both small- and large-scale changes in nutrient availability [*Smith et al.*, 1990; *Gradinger*, 1999, 2008]. However, there is still no clear understanding of the magnitude and variability of ice algal production over most of the Arctic. If we apply knowledge of the controls on small scales and extend tested ice ecosystem models out to larger scales, we can begin to investigate the large-scale variability and fill in the large gaps of information between observations.

[6] Only one model, based on the work of *Arrigo et al.* [1997, 1998], has been used to assess large-scale changes in sea ice primary production [*Arrigo*, 2003]. Although results of the study suggested that snow cover in combination with the proportion of first-year ice may be fundamental in controlling primary production in arctic regions, the model was developed for Antarctic sea ice during 1989–1990 and neglects the important bottom ice community predominant in arctic sea ice. Here we couple the 1-D Physical Ecosystem Model (PhEcoM) ice ecosystem model that has been used to predict sea ice algal biomass and production at individual sites in the Arctic to a global dynamic sea ice model. PhEcoM was tested for first-year pack ice in the seasonal ice zone [*Jin et al.*, 2007, 2009], annual landfast ice [*Jin et al.*, 2006], and multiyear pack ice [*Lee et al.*, 2010]. In this configuration, the prognostic ecosystem model extrapolates detailed information from individual sites to seasonal, regional, and pan-Arctic scales. In this paper, a model run for year 1992 is used to calculate the magnitude and annual cycle of primary production and ice algal biomass within arctic sea ice before recent dramatic sea ice decline. The model simulates sea ice physics and provides external forcing thought to control primary production within sea ice. An additional motivation for this modeling study is the need to include in climate models the role of ice algae in C flux and biogeochemical cycling.

[7] This is the first paper to describe simulated horizontal and annual variability of ice algal production and biomass across the entire Arctic Ocean, including ice-covered arctic shelf seas. Model results are presented and discussed in lieu of sparse observations from the literature, and new insights from analysis of the model results are presented.

2. Model Description

[8] We have coupled a global dynamic/thermodynamic sea ice model, the Los Alamos Sea Ice Model (CICE) [*Hunke and Lipscomb*, 2008; *Hunke and Bitz*, 2009], to the ice ecosystem model of *Jin et al.* [2006]. CICE has been

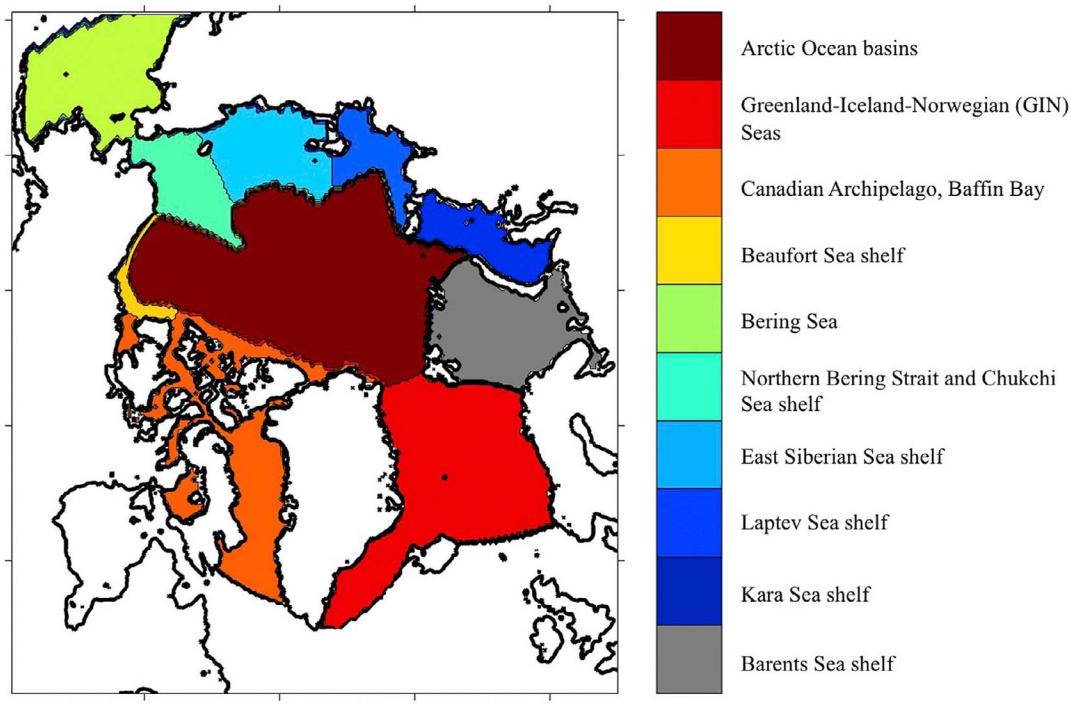

Figure 2. Map of study area showing distribution of the ten study regions: Arctic Ocean basins; Bering Sea; Canadian Archipelago/Baffin Bay (north of 62°N latitude); Greenland-Iceland-Norwegian (GIN) seas; and six pan-Arctic shelf seas (Barents Sea, Kara Sea shelf, Laptev Sea shelf, Eastern Siberian Sea shelf, northern Bering Strait and Chukchi Sea shelf, and Beaufort Sea shelf). The southern boundary of the Arctic Ocean basins region is the shelf edge.

widely used in different ice simulation applications and is extensively documented (see publications in http://climate.lanl.gov/Models/). Currently, CICE partitions the ice pack in each grid cell into a five-category ice thickness distribution, with four ice layers and one snow layer in each category. The horizontal advection of the ecosystem variables is handled like other tracers in CICE. There is a flux exchange of nutrients between ice and ocean as in the work of *Jin et al.* [2006] based on the observations of *Wakatsuchi and Ono* [1983] that brine flux volume in the skeletal layer has a high correlation (R^2 = 0.994) with ice growth rate (dH_{ice}/dt) during the ice growth period. The calculation of the flux is applied in each ice category as a function of bottom sea ice growth/melting rate, temperature and salinity form CICE, and then a sum of the flux from all categories is used to communicate with the ocean. This ice-ocean flux velocity, T*wi* [*Jin et al.*, 2006], is calculated using the same relationship as in the work of *Arrigo et al.* [1993]. Thus the transport of nutrients from the surface ocean is upward during ice growth and when the bottom ice melts, nutrients and algae within the ice are released to the ocean.

[9] The ice ecosystem model is the ice component of PhEcoM, which is shown schematically in Figure 1. The ice component of *Jin et al.* [2006] includes four equations for the four compartments: ice algae, nitrate and ammonium in units of mmol N m^{-3}, and silicate in units of mmol Si m^{-3}. The ice ecosystem model equations are applied to the bottom 3 cm of each ice thickness category in the CICE. *Jin et al.* [2006, 2007] introduce the model equations and parameters, and the history of some improvements. A full set of updated equations and new improvements are summarized and discussed by *Jin et al.* [2008].

[10] CICE was configured with a 20 m slab ocean and run as by *Hunke and Bitz* [2009]. The coupled model was run for year 1992 only, to assess the seasonal to annual ice algal production level. Year 1992 was chosen because its ice extent was consistent with the mean from 1979 to 2000. Key processes important to the functioning of ice algae have been retained from the work of *Jin et al.* [2006], such as (1) nutrient flux between ocean and ice bottom layer and (2) light and nutrient limitation terms of ice algae.

[11] The CICE model domain is global, but this study focuses on the arctic region where ice cover has varied seasonally from 4×10^6 to 16×10^6 km^2 in the last decades. Ice algal carbon contributions and fixation rates are calculated separately for the following ten subregions (Figure 2) to assess regional differences: the Arctic Ocean basins, Bering Sea, northern Bering Strait and Chukchi Sea shelf, Barents Sea shelf, Beaufort Sea shelf, Kara Sea shelf, Laptev Sea shelf, East Siberian Sea shelf, Canadian Archipelago/Baffin Bay (north of 62°N latitude), and Greenland-Iceland-Norwegian (GIN) seas.

[12] The ice ecosystem model component is described in detail by *Jin et al.* [2006]. Ice algae in the model are restricted to the bottom 3 cm of sea ice. The bottom layers of arctic first-year and multiyear ice are the most favorable subhabitat for ice algal blooms [*Gradinger et al.*, 2005; *Gradinger*, 2008]. Chukchi Sea field studies show that

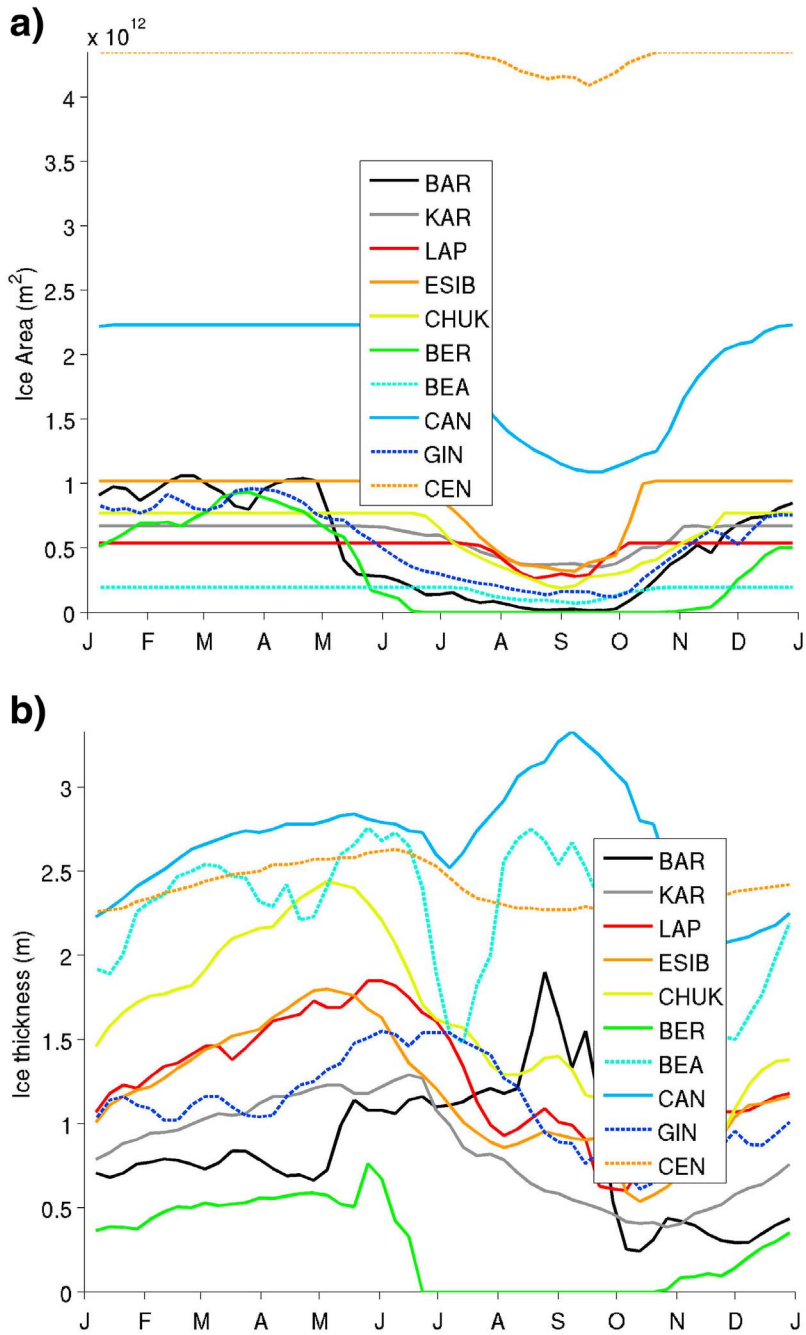

Figure 3. Simulated (a) ice cover area (m^2) and (b) ice thickness (m) in ten study regions. BAR, Barents Sea shelf; KAR, Kara Sea shelf; LAP, Laptev Sea shelf; ESIB, Eastern Siberian Sea shelf; CHUK, northern Bering Strait and Chukchi Sea shelf; BER, Bering Sea; BEA, Beaufort Sea shelf; CAN, Canadian Archipelago/Baffin Bay; GIN, Greenland-Iceland-Norwegian seas; and CEN, Arctic Ocean basins.

"both ice algal pigment concentration and productivity are strongly correlated with the surface nutrient concentration" [*Gradinger*, 2009]. As formulated by *Jin et al.* [2006], the freeze-thaw process drives nutrient transport between the layer of ice containing algae and the underlying ocean. This results in nutrient availability being a function of ice growth/melt rate, which are calculated by CICE. Ice growth and melt rates are explicitly included in the model.

[13] The sea ice model does not include sediments or biology above the bottom 3 cm layer. Consequently, light levels reaching the ice bottom-layer algae in impacted areas may be biased high. There can be widespread occurrence of sediment-laden ice over the Siberian Arctic shelves and similar conditions have been observed covering more than 100,000 km^2 of the Chukchi and Beaufort shelves [*Eicken et al.*, 2005]. Also, freshwater algae growing in the top

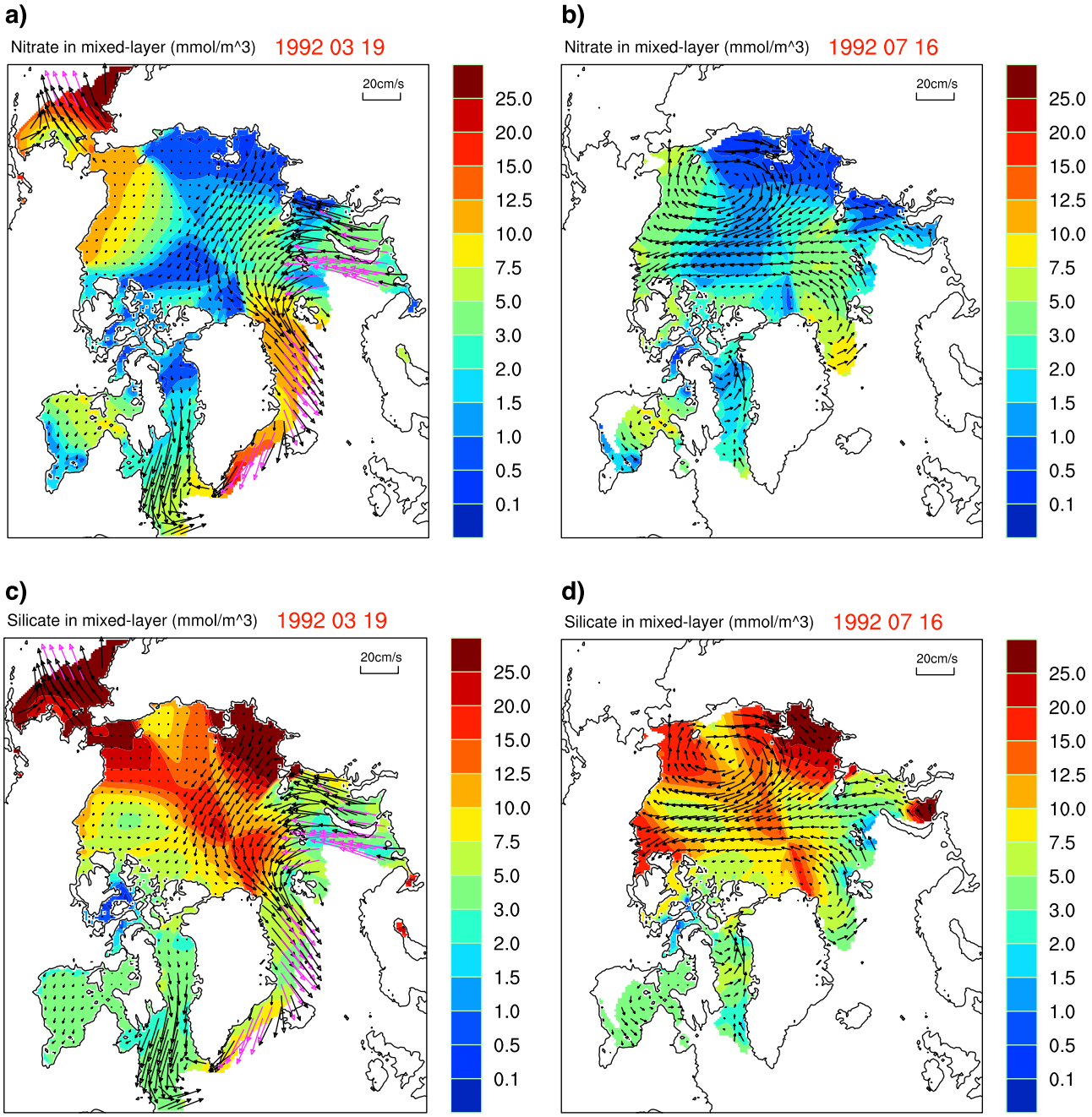

Figure 4. Model ocean mixed layer concentrations (mmol m^{-3}) for nitrate in (a) mid-March and (b) mid-July 1992; and silicate in (c) mid-March and (d) mid-July. Apparent convergence at the North Pole is caused by discontinuities at the pole in the oceanic nutrient forcing data. The white ocean areas indicate open waters. The vector arrows are ocean surface velocity.

layers of the ice can attenuate light in late summer when melt ponds cover large parts of the ice floes [*Gradinger et al.*, 2005]. The sometimes abundant centric diatom suspended from the ice-water interface, *Melosira arctica*, is also of concern, but because of its unpalatability, and very patchy and virtually unknown distribution [*Legendre et al.*, 1992; *Gosselin et al.*, 1997], it is not included in this study.

[14] The initial seawater nitrate and silicate concentrations were set to the World Ocean Atlas 2005 (WOA05) monthly climatology http://www.nodc.noaa.gov/OC5/WOA05/pr_woa05.html and restored on a three-month time scale during the model run.

3. Simulation Results

3.1. Physical and Chemical Environment

[15] During the 1 year model simulation, maximum arctic sea ice area was 15.7×10^6 km^2 in March. The minimum simulated arctic sea ice area was 6.7×10^6 km^2 in September, very close to the 1979–2000 average shown in plots posted

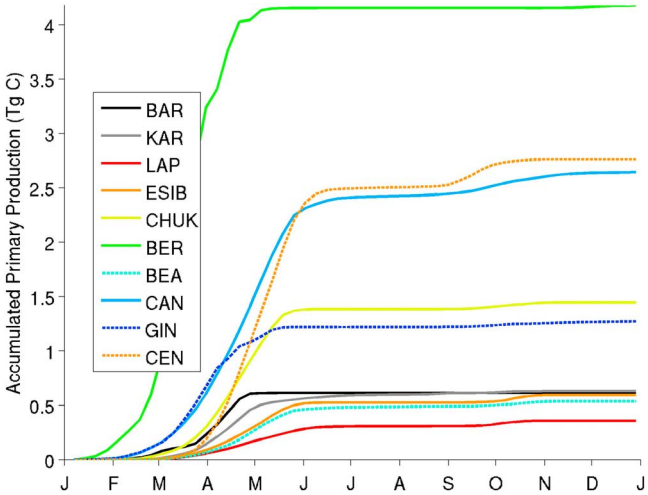

Figure 5. Simulated total primary production within arctic sea ice (Tg C) during 1992. For abbreviations see caption for Figure 3.

by the National Snow and Ice Data Center (http://nsidc.org/). In the simulated time series of sea ice area and thickness for each arctic region, the Arctic Ocean basins and Canadian Archipelago/Baffin Bay stand out in terms of high maximum ice area and thickness (Figures 3a and 3b, respectively). The Beaufort Sea shelf region has the least amount of sea ice cover (0.2×10^{12} m^2) for most of the year, although long winter periods with constant ice area indicate ~100% coverage. All of the ice in the Bering Sea melted by mid-June. In spring, summer and fall, ice was thickest in the Canadian Archipelago/Baffin Bay (up to 3.3 m thick on average) while during November and December the ice was thickest over the Arctic Ocean basins. Before the season of ice melt, the thinnest ice was simulated for the Bering and Barents seas.

[16] Average restored nitrate and silicate concentrations for the middle week of March ranged from, for the most part, several mmol m^{-3} to 25 mmol m^{-3} (Figures 4a and 4c). Values above 20 mmol N m^{-3} were found only in the western Bering Sea. The overall spatial pattern of modeled nutrient concentrations under the ice from spring through summer changed little from month to month. For comparison, the nutrient distributions for July are shown in Figures 4b and 4d. This consistency was as expected since most of the depletion of nutrients occurs when the ice is gone (R. Gradinger, personal communication, 2006).

3.2. Ice Algal Production and Biomass

[17] Simulated sea ice primary production for the pan-Arctic was 15.1 Tg C yr^{-1}. The most productive regions were the Bering Sea (4.2 Tg C yr^{-1}), Arctic Ocean basins (2.8 Tg C yr^{-1}) and Canadian Archipelago/Baffin Bay (2.7 Tg C yr^{-1}; Figure 5). Other significant fractions were the northern Bering Strait and Chukchi Sea shelf (1.3 Tg C yr^{-1}) and GIN Seas (1.2 Tg C yr^{-1}). The remaining five pan-Arctic shelf regions (i.e., Barents Sea shelf, Beaufort Sea shelf, Kara Sea shelf, Laptev Sea shelf, East Siberian Sea

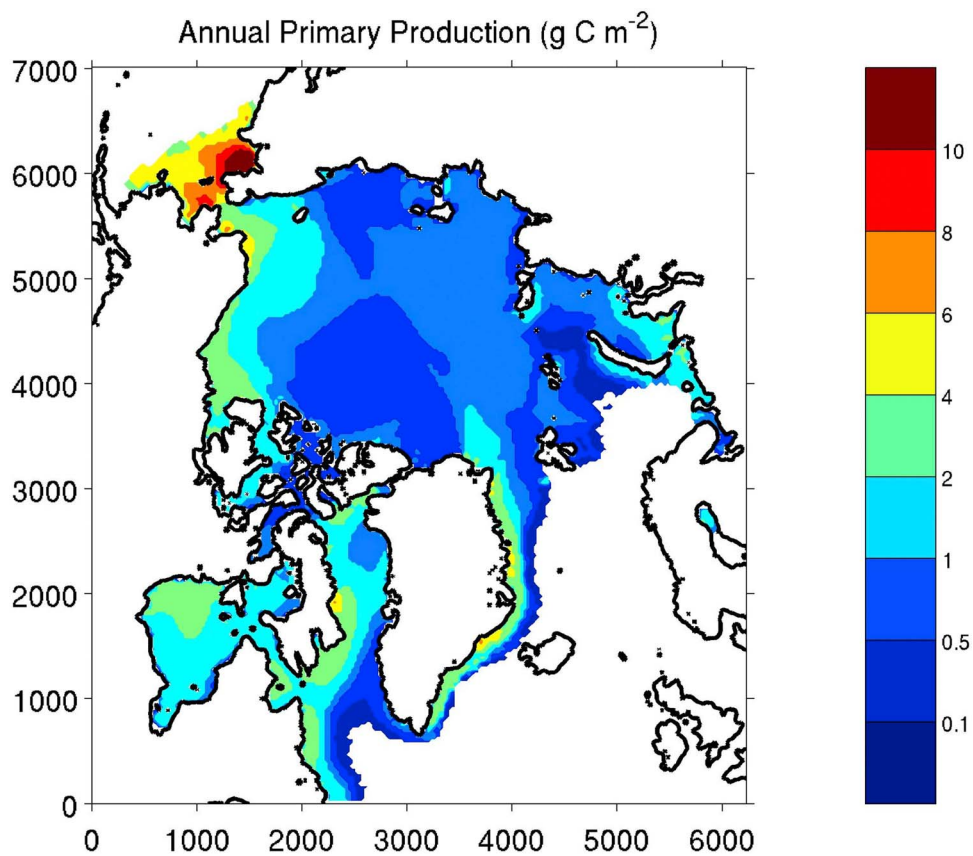

Figure 6. Map of total annual primary production within arctic sea ice simulated for 1992.

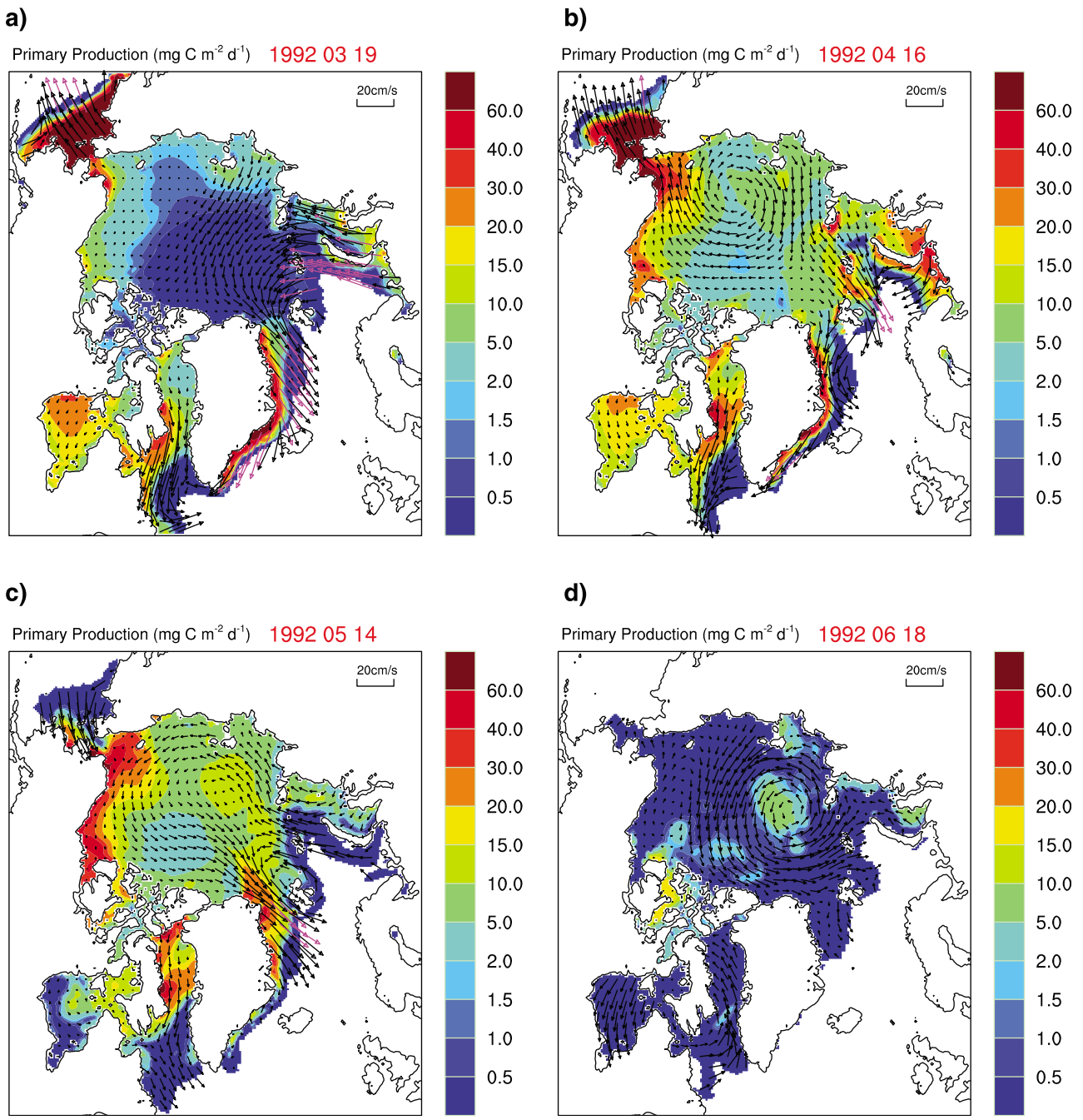

Figure 7. Maps of simulated rates of ice algal production in the middle of (a) March, (b) April, (c) May, and (d) June 1992 and sea ice algal biomass distribution in the middle of (e) March, (f) April, (g) May, and (h) June 1992. The vector arrows are ice velocity.

shelf) contributed each ≤5% to the total arctic sea ice primary production in 1992. Most of the pan-Arctic production occurred in March (3.6 Tg C), April (3.8 Tg C), and May (3.0 Tg C).

[18] A pan-Arctic view map shows the spatial distribution of simulated total ice primary production for year 1992 (Figure 6). Annual areal sea ice primary production was as high as 10 g C m^{-2} in the Bering Sea. High values (>2 g C m^{-2}) were simulated in coastal regions and the lowest values in the vicinity of the Beaufort Gyre and Transpolar Drift System, and over much of the Russian shelves. The Beaufort Gyre and the Transpolar Drift System, or Stream, are the two primary components of the wind-driven arctic ice circulation pattern. The Beaufort Gyre is a clockwise circulation in the Beaufort Sea well beyond the shelf, north of Alaska. The Transpolar Drift carries ice that moves from the Siberian coast, across the pole and then exits the Arctic east of Greenland.

[19] The horizontal distributions of average daily production rates for the middle of March, April, May, and June, (Figures 7a–7d) are similar to the patterns displayed with ice algal biomass concentrations (Figures 7e–7h). The ice algal standing stocks display less biomass in mid-June at most

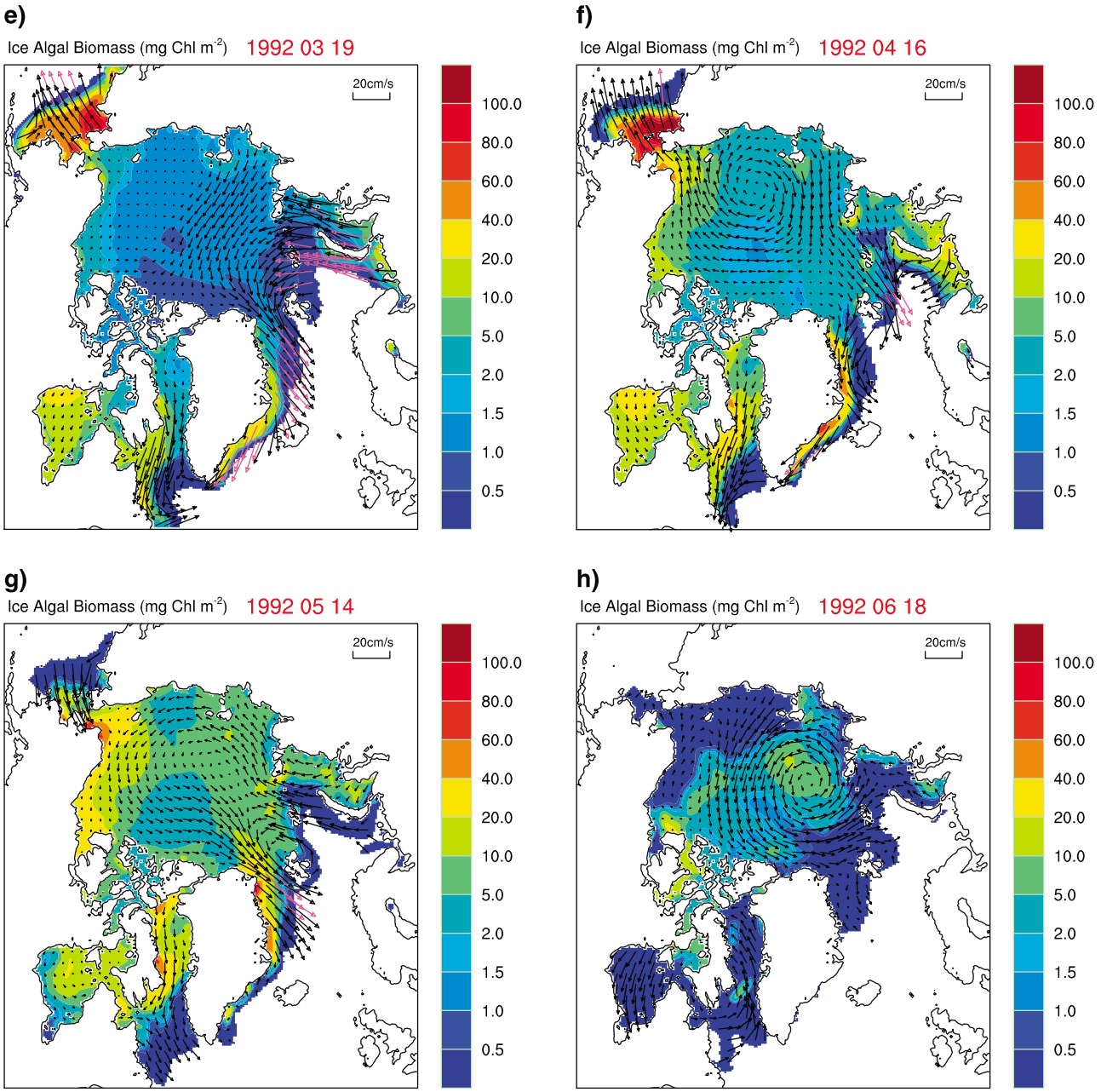

Figure 7. (continued)

locations as compared to mid-May and a continued decrease in biomass across the entire Arctic from mid-June to mid-July. The simulated production rates follow the same trend, with an even more dramatic decline between mid-May and mid-June leading to very low rates of production in July.

[20] Averaged over the ice area, simulated ice algal production rates (Figure 8a) and ice algal biomass (Figure 8b) were maximum in the Bering Sea where the daily production rate peaked at 100 mg C m^{-2} d^{-1} and the weekly mean chlorophyll a (Chl) concentration was above 60 mg Chl m^{-2}. In the Arctic Ocean basins, ice algal biomass and production maxima were much lower; only as high as 8 mg Chl m^{-2} and 10 mg C m^{-2} d^{-1}, respectively. Elsewhere in the Arctic, maxima in simulated ice algal daily production rates and weekly mean ice algal biomass ranged from 7 to 48 mg C m^{-2} d^{-1} and 6 to 32 mg Chl m^{-2}, respectively. In midsummer, from July through the first half of August, simulated ice algal biomass was up to around 3 mg Chl m^{-2} in the little ice that remained in the Beaufort Sea shelf. Elsewhere, the ice algal biomass was mostly less than 1 mg Chl m^{-2}, with slightly higher values in the Laptev Sea shelf and Canadian Archipelago/Baffin Bay.

[21] Intense seasonal variability of ice algal biomass within arctic sea ice is displayed in the latitude-time plot of the model results (Figure 9). The plot shows ice algal biomass starting to accumulate before March below 75° latitude, as

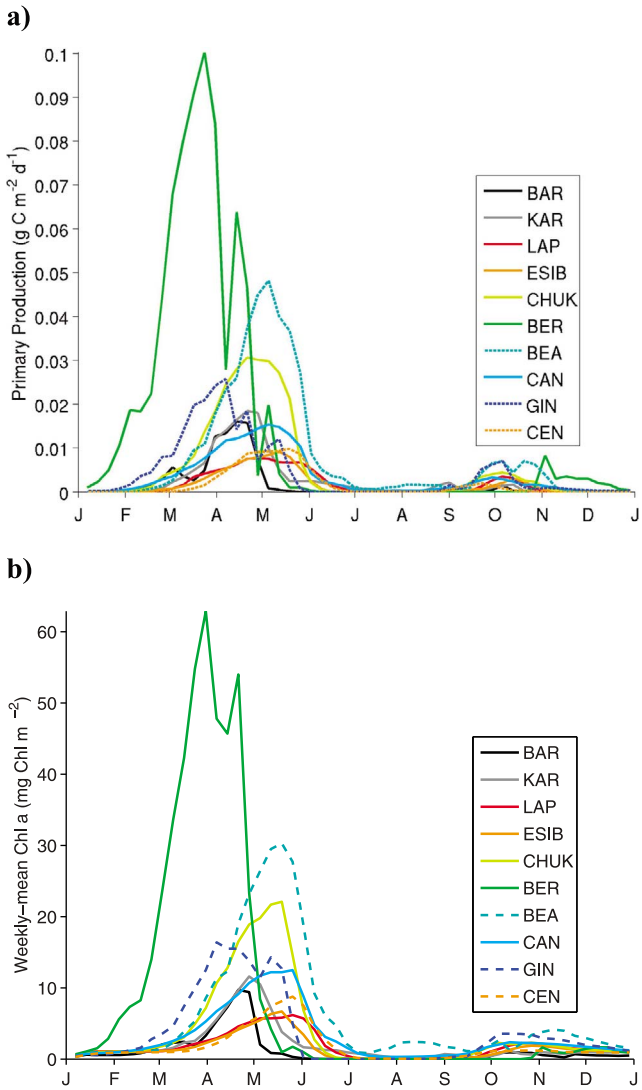

Figure 8. Simulated mean (a) daily rate of ice primary production and (b) ice algal biomass averaged over ice area in the ten study regions during 1992. For abbreviations see caption of Figure 3.

well as a second pulse beginning in September at high latitudes, and progressing to lower latitudes over the next 3 months. Maximal latitude-averaged concentrations reach 40 mg Chl m^{-2} and 10 mg Chl m^{-2} in the spring and fall, respectively. In summer (June, July and August), when there is little ice remaining below 70° latitude, the latitude-averaged ice algal biomass generally does not exceed 5 mg Chl m^{-2} and is for the most part no higher than 1 mg Chl m^{-2}. Average ice algal standing stock in September is relatively low compared to the ice algal standing stock in the springtime (Figure 9; see also Figure 8b). According to the model results, approximately 8% of total primary production within arctic sea ice may occur during autumn (September, October, and November).

4. Discussion

[22] Physical and chemical variables such as per cent ice cover, ice thickness, and nutrient concentrations can vary substantially on regional and seasonal scales, as displayed in the model results (Figures 3 and 4). On small scales, it is relatively well established that light availability (i.e., ice thickness, snow depth), and nutrient supplies place the strongest controls on ice algal growth [*Lavoie et al.*, 2009; *Jin et al.*, 2006]. The influence of physical and chemical variables on large-scale sea ice biomass and production are examined here in a qualitative sense. First, pan-Arctic ice algal production and biomass within sea ice, and their large scale-spatial and temporal variability are discussed. Following, the discussion focuses in on specific subregions before extending back out again to the pan-Arctic scale and possible consequences of a warming Arctic.

4.1. Pan-Arctic Perspective of Sea Ice Algal Production

[23] The simulated sea ice primary production of 15.1 Tg C yr^{-1} for the Arctic Ocean and surrounding marginal seas (including the Bering Sea) is at the low end of the range of 9–73 Tg C yr^{-1} estimated by *Legendre et al.* [1992]. They used a nominal ice algal production value of 10 g C m^{-2} yr^{-1} over the annual pack ice (7×10^6 km^2) and 0.6 g C m^{-2} yr^{-1} for the multiyear ice (5×10^6 km^2). Their lower limit was calculated using the annual ice area of 0.6×10^6 km^2 of *Subba Rao and Platt* [1984] instead of the more extensive 7×10^6 km^2. One reason our model results are at the low end of the range of estimates based on observations is that the model does not include the centric diatom *Melosira arctica*, which suspends in strands from the bottom of sea ice. Because their distribution is very patchy and largely unknown, it is not possible at this point in time to realistically model and validate this subice algal species.

4.2. Spatial Variability of Ice Algal Biomass and Production

[24] In the model, the Arctic Ocean basins and the Bering Sea form the largest portions of primary production within arctic sea ice for different reasons (see Figure 5). In the Arctic Ocean basins, large annual ice area and duration (Figure 3a) compensate for the low rates of primary production (>90% of area less than 2 mg C m^{-2} yr^{-1}; see Figure 4). It is the opposite case in the Bering Sea, where ice covers an area of only about one-fifth of that over the Arctic Ocean basins before it completely melts away in early June. Simulated annual primary production is highest in the Bering Sea, ranging from 2 g C m^{-2} up to 10 g C m^{-2}. The Canadian Archipelago/Baffin Bay lies between both extremes in ice coverage and productivity with annual primary production mostly between 1 and 4 mg C m^{-2}. It ranks a close third in the portion of primary production within arctic sea ice because of its relatively large ice area (compared to other ice-covered shelf sea regions), which ranges throughout the year between a quarter and a half that of the Arctic Ocean basins. To varying degrees, the interplay between ice cover and rates of primary production appear to determine the total annual sea ice primary production over arctic seas.

[25] The order of magnitude range of simulated ice algal biomass is in general agreement with the compilation of in situ measurements for the Arctic [*Arrigo*, 2003]. Maximum Chl biomass observed within arctic bottom ice are reported by *Arrigo* [2003] to range from 5 to 160 mg Chl m^{-2}. In comparison, model results show highest weekly mean Chl biomass peaking at approximately 7 mg Chl m^{-2}

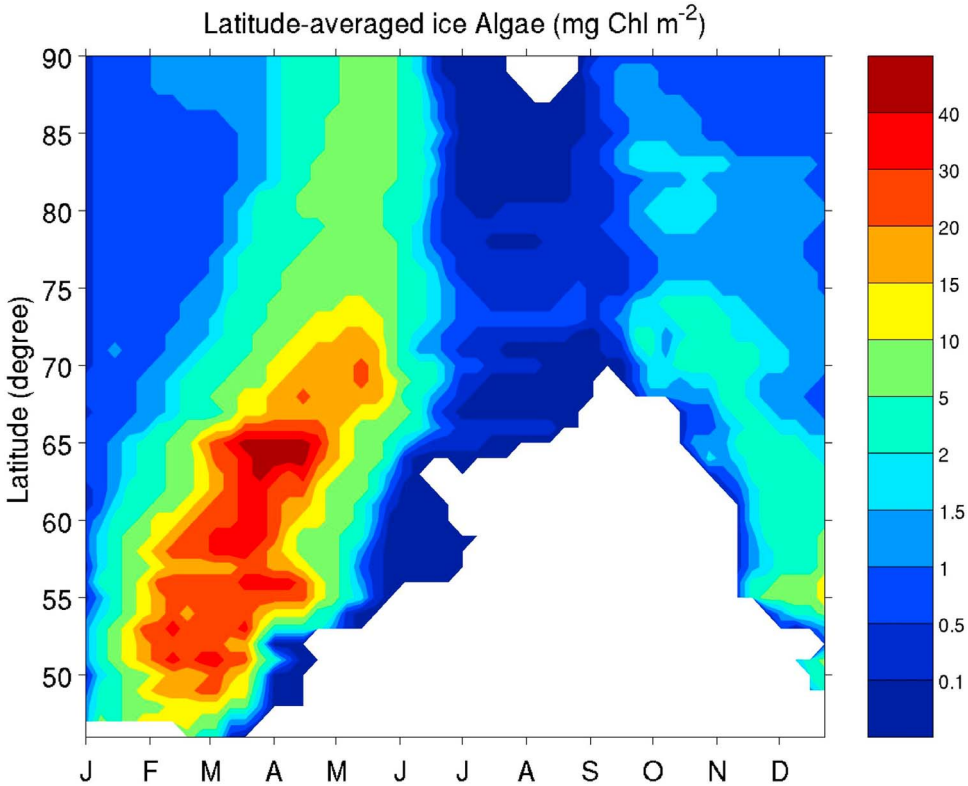

Figure 9. Latitude-averaged ice algal biomass simulated during 1992.

in the Laptev Sea shelf to 64 mg Chl m^{-2} in the Bering Sea (Figure 8b).

[26] For the most part, regional patterns of observed ice algal biomass are seen in the model results. Observations of ice algal biomass in arctic coastal waters are generally higher than those from the deep Arctic Ocean basins and the model results reflect this (Figures 7e–7g). Biomass values above 70 mg Chl m^{-2} have been observed along the North American coast [*Gradinger*, 2008, and references therein]. These maxima are relatively high compared to values up to only a few mg Chl m^{-2} for bottom ice in the permanently ice-covered Arctic Ocean [*Gosselin et al.*, 1997], and about 2 mg Chl m^{-2} in the Transpolar Drift System and the Beaufort Gyre [*Gradinger*, 1999; *Gradinger et al.*, 2005]. Model results for these central arctic areas do not exceed 3 mg Chl m^{-2} for the summer season sampled (July-October; Figure 8b).

[27] Large-scale regional differences of surface ocean layer nutrient distribution reflect the large-scale regional production and biomass seen in observations [*Gradinger*, 2009], and for this study, the model results as well. For the model study comparisons we have focused on nitrate concentrations because several studies indicate that the availability of nitrate in the surface water limits the accumulation and productivity of bottom ice algae during the spring bloom in arctic waters [*Gradinger*, 2009; *Rózanska et al.*, 2009, and references therein]. The integrated Chl concentrations above 70 mg Chl m^{-2} simulated along the North American coastline and lower biomass in pack ice of the oligotrophic Arctic basin have been observed for all seasons [*Gradinger*, 2009, and references therein). Because the overall spatial pattern of modeled nitrate concentrations under the ice from March through summer changed little from month to month (model results not shown), March (i.e., wintertime) nitrate concentrations were used for the under ice nitrate concentration comparisons. Comparisons of restored wintertime surface ocean layer nitrate concentrations (Figure 4a) with simulated springtime sea ice biomass (Figures 7e and 7f) and rate of primary production (Figures 7a and 7b) reveal a similar spatial pattern. That is, the magnitude of nutrient concentration corresponds roughly to the relative amount of biomass and rate of daily production. The highest biomass and production is found in the western Bering Sea where the nitrate concentrations are the highest. Relatively high values are also found in coastal regions where nitrate concentrations are also high.

[28] Although in general, the regional patterns of ice algal biomass and productivity mimic each other and those of seawater nitrate concentration, they are not an exact fit. Deviations suggest nutrient supply is not the only factor controlling ice algal growth. For example, high seawater nitrate concentrations are modeled east of Greenland (Figure 4a), but only the band of ice along the coast exhibits high productivity and biomass because it is not as susceptible to melting as ice over the warm waters on the east side of the Fram Strait. Sea ice algal release into the water column from bottom ice melting introduces a loss term that is as variable as the ice melt rate on which its parameterization is based. Sudden pulses of sea ice algal release have been observed on local scales [*Jin et al.*, 2006; *Michel et al.*, 2006]. On somewhat larger scales, this phenomenon could also account for the dissimilarities between spatial patterns of ice algal biomass and productivity, and seawater nitrate concentrations.

[29] Another explanation for differences in the spatial patterns is the springtime highs in productivity (i.e., >20–30 mg C m^{-2} d^{-1}) and biomass (i.e., >10–20 mg Chl m^{-2}) in the Canadian Beaufort Sea and Baffin Bay (Figures 7a, 7b, 7e, and 7f), where nitrate concentrations are low (<2 mmol m^{-3}) and ice growth rates are high (data not shown). High ice growth rates are plausible in the model along the Beaufort coast where ice growth is continuous because of offshore winds blowing ice away from the coast and new ice forming in its place. The model results suggest that when ice growth rates are consistently high, this may be enough to ensure sufficient nutrient availability and, hence, enhanced productivity and biomass accumulation, even when nutrient supplies in the seawater are low.

[30] The relatively high simulated values of ice algal biomass and productivity beyond the shelf in the Alaskan Beaufort Sea (Figures 7a and 7b) are not supported by the observations of *Gradinger* [2009]. Between 10 May and 8 June, *Gradinger* [2009] measured low values for the low-nutrient Alaskan Beaufort Sea, and much higher ice algal biomass and rates of production in the Chukchi Sea shelf where nutrients were high. Although the comparison is between model results and observations are about 20 years apart, this lack of agreement appears to be due to uniformly high climatological seawater nitrate concentrations (5 to 12.5 mmol m^{-3}) over the entire Alaskan Beaufort Sea shelf and much of the Chukchi Sea shelf (Figure 4a). The disparity highlights the shortcomings of restoring to a nutrient climatology that is based on very few observations and cautions the use of limited, site-specific observations to evaluate large-scale model results. A nutrient climatology of known and adequate quality to initialize the model and evaluate restored nutrient concentrations is critically needed for the entire Arctic.

4.3. Annual Cycle of Sea Ice Primary Production and Biomass

[31] The earlier ice algal bloom occurs in the Bering Sea because of higher light intensities early in the year. Productivity in this region is enhanced because of the high seawater nitrate concentrations ranging from 5 to 25 μM nitrate. The beginning of ice algal growth at the base of the ice with the spring increase in solar radiation [*Horner*, 1985] is reflected in the time delay of the simulated blooms with increasing latitude (Figure 9).

[32] There are few time series observations to verify the peaks in the simulated annual cycles of ice algal biomass and productivity (Figures 8a and 8b). Most of the observations reported in the literature for the central Arctic have been conducted in late-summer or autumn when accessible by ship. Our model results suggest that the bloom period in the central Arctic occurs well before July. Ice algae from a few landfast ice sites have been studied intensively for several spring field seasons, including the Barrow Strait (74°40′N) in the center of the Northwest Passage; and Chukchi Shelf near Barrow, Alaska, (71°20′N). The bloom periods extended from mid-March to Mid-June for the high arctic sites [*Cota et al.*, 1991], and from March to mid-May on the Chukchi shelf [*Jin et al.*, 2006], in good agreement with the modeled bloom periods. As for the timing of ice algal release, *Michel et al.* [2006] report that it typically occurs at the end of May or early June in the Canadian Archipelago/Baffin Bay. This coincides with the time of decreasing Chl concentration in the model results (Figure 8b).

[33] There is a dramatic drop in simulated ice algal productivity across the Arctic from mid-May to mid-June (Figures 7b and 7c) when the average arctic ice growth rate reaches its annual minimum (Figure 10). Since nutrient supply is driven by ice growth rate in the model, slower ice growth means fewer nutrients available. The coincidentally low productivity suggests nutrient limitation of ice algal growth. Indeed, after sufficient light triggers the vernal ice algal bloom, the declining average ice algal growth rate roughly parallels the decreasing average ice growth rate. In a similar manner, the dramatic drop in ice algal productivity is followed by an almost parallel decline in ice algal biomass a couple of weeks later. This delay can be seen for each region as well (Figures 8a and 8b). For example, maximum weekly mean Chl concentrations for the Beaufort Sea and Chukchi Sea shelves occur in the middle of May, and in the Canadian Archipelago/Baffin Bay at the end of May, both after the decline in productivity beginning in early May. Within one month, ice algal biomass can drop from tens of mgs Chl m^{-2} to less than 1 mg Chl m^{-2} over large areas (compare Figures 7f and 7g). The decline coincides with the release of the ice algae into the water column because of bottom ice melting. Average ice algal productivity falls to its lowest value in early July when the average bottom ice melting rate peaks (Figure 10).

[34] A significant spike in productivity appears at the time of ice regrowth after the summer melt season in the model results (Figures 8a, 9, and 10). This happens before light intensities lessen because of snow accumulation and increasing ice thickness. It is unclear how important ice algal growth is in the autumn. On the basis of the model results, ice algal growth during this period contributes as much as 8% of the total primary production within arctic sea ice.

4.4. Estimates of Regional Annual Production of Arctic Ice Algae

[35] Simulated annual sea ice primary production for the ten delineated arctic subregions (Figure 2) are listed in Table 1, along with literature estimates based on observations. In most cases, the simulated production is comparable to observed. A notable exception is the East Siberian Sea. Here the nutrient climatology used to initialize the model is based on very few field data and results in low-nitrate concentrations restored for this shelf region that are not sufficient to support annual production much above 0.6 g C m^{-2} as compared to 4.7 g C m^{-2} estimated by *Petrova et al.* [2004].

[36] The model estimate of 1.5 g C m^{-2} yr^{-1} for sea ice primary production in the Chukchi Sea shelf agrees remarkably well with the annual estimated range of 1–2 g C m^{-2} based on measurements in May/June 2002 [*Gradinger*, 2009]. High ice algal productivity in the Chukchi Sea requires substantial nutrient reservoirs which are supplied by high-nutrient Pacific water that flows through the Bering Strait. The relatively high modeled nutrient concentrations in the Chukchi Sea shelf (Figures 4a and 4b) reflect the transport of nutrient rich waters that support the high ice algal productivity.

[37] An important characteristic of the Bering and Chukchi seas is their high biological productivity. As discussed

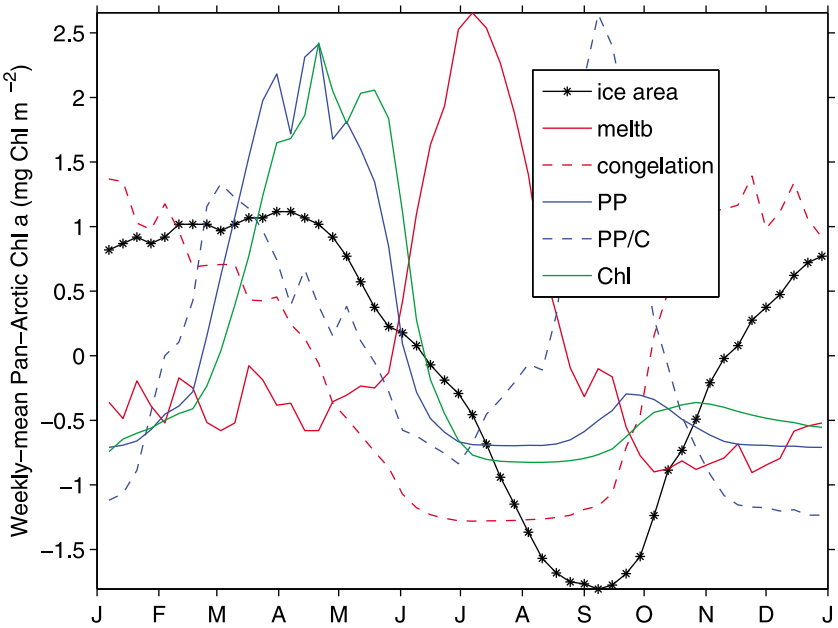

Figure 10. Ice area, bottom ice melt rate (meltb), ice growth rate (congelation), primary productivity (PP), specific ice algal growth rate (PP/C), and ice algal biomass (Chl) for the entire arctic region normalized by subtracting the mean and then dividing by the standard deviation.

earlier, the largest fraction of annual primary production within arctic sea ice was stimulated in the Bering Sea because of high rates of primary production. Although the modeled rates of primary production in the Bering Sea are higher than in situ measurements, they are the same order of magnitude [*Alexander and Chapman*, 1981]. Furthermore, literature estimates of sea ice primary production in the Bering Sea are based on very limited sampling [*Alexander and Chapman*, 1981; *McRoy and Goering*, 1974]. Our model results suggest that considerably more organic C is produced in Bering Sea ice.

[38] Because of the inaccessibility of the Russian shelves and extremely remote ice environments, virtually no information on sea ice algal productivity is available for these areas. For example, we know of no literature estimates of the annual production of sea ice algae from the Kara Sea shelf, Laptev Sea shelf, and GIN Seas. The model results suggest that these regions are critical habitats for algae living within sea ice (Figures 6 and 7a). To evaluate these findings and understand the implications of future sea ice loss, we need a baseline of observations on which to gauge change.

4.5. Significance of the Timing and Variations of Ice Algal Release Into Water

[39] As the Arctic warms, large-scale patterns of ice algal biomass will change because of changes in the seasonality and spatial variability of nutrient supply, sea ice growth, and sea ice melt, as revealed from this modeling study. These physical processes indirectly affect the sea ice, pelagic, and benthic grazers by influencing total ice primary production and release of ice algae to the water column. A sufficient nutrient supply at the ocean surface is needed to sustain ice

Table 1. Arctic Sea Ice Primary Production Averaged Over Ice Area in the Ten Study Regions (g C m^{-2} yr^{-1}) and for the Total Arctic (Tg C yr^{-1})

Arctic Subregion	Value	Reference, Comment	This Study Value
Arctic Ocean Basins	6[a]	*Gosselin et al.* [1997]	2.8
Bering Sea	0.2–1.5	*Alexander and Chapman* [1981]	4.2
	0.2–0.4	*McRoy and Goering* [1974]	
Chukchi Sea shelf	1–2	*Gradinger* [2009]	1.5
Barents Sea	0.2–5.3[a]	*Hegseth et al.* [1998]	0.6
	1.5	*Vetrov and Romankevich* [2004]	
Beaufort Sea	0.7	*Horner and Schrader* [1982], nearshore	0.5 (shelf)
Kara Sea	—	—	0.6
Laptev Sea	—	—	0.4
East Siberian Sea	4.7	*Petrova et al.* [2004]	0.6
Canadian Arctic	5	*Bergmann et al.* [1991], Barrow Strait area	2.7 (>62°N)
GIN Seas	—	—	1.3
Total Arctic	6 9–70	*Subba Rao and Platt* [1984], young ice *Legendre et al.* [1992]	15.1

[a]These values include estimated production from subice algae in addition to ice bottom algae.

algal growth. However, high-nutrient concentrations alone may not support high ice algal growth. The model results suggest that ice growth is required to transport the nutrients from the surface ocean to the bottom ice algal habitat.

[40] An earlier and/or faster ice melt would lead to earlier ice melting, a shortened production season, and likely less production. If ice algal release to the water column happens when there are few grazers to recycle the C within the water column, more will be transferred to the benthos or exported to deep waters. A delay of only a few days may be critical. Even though ice algal production can be smaller than subsequent phytoplankton production, vertical export has been shown to be significant [*Michel et al.*, 2006]. The springtime carbon budget of sea ice algae of *Michel et al.* [1996] provides evidence that the timing of the process that drives the ice algal release from the ice bottom, more than the period of algal production, is critical in determining whether pelagic consumers are supplied with food at a period of the year when no other food sources are available.

5. Conclusion

[41] By coupling an ice ecosystem model with the global dynamic/thermodynamic sea ice model, CICE, we have developed a predictive tool for estimating the temporal and spatial variability of sea ice algae in arctic regions where data are very sparse. The model results agree reasonably well with the limited observations that are available, suggesting that the physical processes important to ice algal growth and release on large scales are included in the model with adequate fidelity.

[42] Model results indicate that the area and duration of sea ice cover outweigh transient pulses in productivity for determining the annual primary production within arctic sea ice. Ice growth is needed for transporting nutrients to the bottom ice algal subhabitat and to sustain the bloom. In general, high ice algal biomass and productivity correspond to high surface seawater nutrient concentrations. However, an exceptionally high ice growth rate and continuous ice growth, even when seawater nutrient concentrations are relatively low, can enhance productivity and ice algal accumulation.

[43] Gridded data of acceptable quality are critical for the large-scale modeling of algal biomass and productivity within arctic sea ice. Immediate observational data needs include more extensive seawater nutrient concentrations for model initialization, and in-ice carbon uptake rates and Chl concentrations for model evaluation.

[44] This modeling study suggests that ice algal release is sudden and rapid over large areas of the Arctic because of bottom ice melt. On large spatial and temporal scales, nutrient supply, ice growth rate and ice melt determine the amount and timing of fixed C released into the water column. This supply of organic matter goes on to impact the water column food web of polar seas, its spatial variability, and its potential response to global climate change.

[45] **Acknowledgments.** This work was supported mostly by funding through the DOE EPSCoR program, grant DE-FG02-08ER46502. Partial support was provided under the IARC/JAMSTEC Cooperative Research Agreement and NSF ARC-0652838. We also thank the two anonymous reviewers for their helpful comments.

References

Alexander, V., and T. Chapman (1981), The role of epontic algal communities in Bering Sea ice, in *The Eastern Bering Sea Shelf: Oceanography and Resources*, edited by D. W. Hood and J. A. Calder, pp. 773–780, Univ. of Wash. Press, Seattle.

Arrigo, K. R. (2003), Primary production in sea ice, in *Sea Ice: An Introduction to Its Physics, Biology, Chemistry and Geology*, edited by D. N. Thomas and G. S. Dieckmann, pp. 143–183, Blackwell Sci., Oxford, U. K.

Arrigo, K., J. N. Kremer, and C. W. Sullivan (1993), A simulated Antarctic fast ice ecosystem, *J. Geophys. Res.*, *98*, 6929–6946, doi:10.1029/93JC00141.

Arrigo, K. R., D. L. Worthen, M. P. Lizotte, P. Dixon, and G. Dieckmann (1997), Primary production in Antarctic sea ice, *Science*, *276*, 394–397, doi:10.1126/science.276.5311.394.

Arrigo, K. R., D. L. Worthen, A. Schnell, and M. P. Lizotte (1998), Primary production in Southern Ocean waters, *J. Geophys. Res.*, *103*, 15,587–15,600, doi:10.1029/98JC00930.

Bergmann, M. A., H. E. Welch, J. E. Butler-Walker, and T. D. Silfred (1991), Ice algal photosynthesis at Resolute and Saqvaqjuac in the Canadian Arctic, *J. Mar. Syst.*, *2*, 43–52, doi:10.1016/0924-7963(91)90012-J.

Caroll, M. L., and J. Caroll (2003), The Arctic seas, in *Biogeochemistry of Marine Systems*, edited by K. D. Black and G. B. Shimmield, pp. 127–156, Blackwell Sci., Boca Raton, Fla.

Cota, G. F., L. Legendre, M. Gosselin, and R. G. Ingram (1991), Ecology of bottom ice algae: I. Environmental controls and variability, *J. Mar. Syst.*, *2*, 257–277, doi:10.1016/0924-7963(91)90036-T.

Eicken, H., R. Gradinger, A. Gaylord, A. Mahoney, I. Rigor, and H. Melling (2005), Sediment transport by sea ice in the Chukchi and Beaufort Seas: Increasing importance due to changing ice conditions?, *Deep Sea Res., Part II*, *52*, 3281–3302, doi:10.1016/j.dsr2.2005.10.006.

Gosselin, M., M. Levasseur, P. A. Wheeler, R. A. Horner, and B. C. Booth (1997), New measurements of phytoplankton and ice algal production in the Arctic Ocean, *Deep Sea Res., Part II*, *44*, 1623–1644, doi:10.1016/S0967-0645(97)00054-4.

Gradinger, R. (1999), Vertical fine structure of algal biomass and composition in Arctic pack ice, *Mar. Biol. Berlin*, *133*, 745–754, doi:10.1007/s002270050516.

Gradinger, R. (2008), Sea ice, in *Arctic Ocean Synthesis: Analysis of Climate Change Impacts in the Chukchi and Beaufort Seas With Strategies for Future Research*, edited by R. Hopcroft, B. Bluhm, and R. Gradinger, project 503 (S00006183), pp. 24–32, Inst. of Mar. Sci., Univ. of Alaska Fairbanks, Fairbanks.

Gradinger, R. (2009), Sea-ice algae: Major contributors to primary production and algal biomass in the Chukchi and Beaufort Seas during May/June 2002, *Deep Sea Res., Part II*, *56*, 1201–1212, doi:10.1016/j.dsr2.2008.10.016.

Gradinger, R. R., K. Meiners, G. Plumley, Q. Zhang, and B. A. Bluhm (2005), Abundance and composition of the sea-ice meiofauna in offshore pack ice of the Beaufort Gyre in summer 2002 and 2003, *Polar Biol.*, *28*, 171–181, doi:10.1007/s00300-004-0674-5.

Hegseth, E. N. (1998), Primary production of the northern Barents Sea, *Polar Res.*, *17*, 113–123, doi:10.1111/j.1751-8369.1998.tb00266.x.

Horner, R. (Ed.) (1985), *Sea Ice Biota*, CRC Press, Boca Raton, Fla.

Horner, R., and G. C. Schrader (1982), Relative contribution of ice algae, phytoplankton, and benthic microalgae to primary production in nearshore regions of the Beaufort Sea, *Arctic*, *35*, 485–503.

Hunke, E. C., and C. M. Bitz (2009), Age characteristics in a multidecadal Arctic sea ice simulation, *J. Geophys. Res.*, *114*, C08013, doi:10.1029/2008JC005186.

Hunke, E. C., and W. H. Lipscomb (2008), CICE: The Los Alamos Sea Ice Model, documentation and software, version 4.0., *Tech. Rep. LA-CC-06-012*, Los Alamos Natl. Lab., Los Alamos, N. M. (Available at http://climate.lanl.gov/Models/CICE/index.htm.)

Jin, M., C. J. Deal, J. Wang, K.-H. Shin, N. Tanaka, T. E. Whitledge, S. H. Lee, and R. Gradinger (2006), Controls of the land fast ice-ocean ecosystem offshore Barrow, Alaska, *Ann. Glaciol.*, *44*, 63–72, doi:10.3189/172756406781811709.

Jin, M., C. Deal, J. Wang, V. Alexander, R. Gradinger, S. Saitoh, T. Iida, Z. Wan, and P. Stabeno (2007), Ice-associated phytoplankton blooms in the southeastern Bering Sea, *Geophys. Res. Lett.*, *34*, L06612, doi:10.1029/2006GL028849.

Jin, M., C. J. Deal, and J. Wang (2008), A coupled ice-ocean ecosystem model for 1-D and 3-D applications in the Bering and Chukchi Seas, *Chin. J. Polar Sci.*, *19*(2), 218–229.

Jin, M., C. J. Deal, J. Wang, and C. P. McRoy (2009), Response of lower trophic level production to long-term climate change in the southeastern Bering Sea, *J. Geophys. Res.*, *114*, C04010, doi:10.1029/2008JC005105.

Lavoie, D., K. Denman, and C. Michel (2005), Modeling ice algal growth and decline in a seasonally ice-covered region of the Arctic (Resolute Passage, Canadian Arctic), *J. Geophys. Res.*, *110*, C11009, doi:10.1029/2005JC002922.

Lavoie, D., R. W. Macdonald, and K. Denman (2009), Primary productivity and export fluxes on the Canadian shelf of the Beaufort Sea: A modeling study, *J. Mar. Syst.*, *75*, 17–32, doi:10.1016/j.jmarsys.2008.07.007.

Lavoie, D., K. L. Denman, and R. W. Macdonald (2010), Effects of future climate change on primary productivity and export fluxes in the Beaufort Sea, *J. Geophys. Res.*, *115*, C04018, doi:10.1029/2009JC005493.

Lee, S., M. Jin, and T. E. Whitledge (2010), Comparison of bottom sea-ice algal characteristics from coastal and offshore regions in the Arctic Ocean, *Polar Biol.*, *33*, 1331–1337, doi:10.1007/s00300-010-0820-1.

Legendre, L., S. F. Ackley, G. S. Dieckmann, B. Gullicksen, R. Horner, T. Hoshiai, I. A. Melnikov, W. S. Reeburgh, M. Spindler, and C. W. Sullivan (1992), Ecology of sea ice biota: Part 2. Global significance, *Polar Biol.*, *12*, 429–444.

McRoy, C. P., and J. J. Goering (1974), The influence of ice on the primary productivity of the Bering Sea, in *Oceanography of the Bering Sea*, *With Emphasis on Renewable Resources*, edited by D. W. Hood and E. J. Kelley, pp. 403–421, Inst. Mar. Sci., Univ. of Alaska Fairbanks, Fairbanks.

Michel, C., L. Legendre, R. G. Ingram, M. Gosselin, and M. Levasseur (1996), Carbon budget of sea-ice algae in spring: Evidence of a significant transfer to zooplankton grazers, *J. Geophys. Res.*, *101*, 18,345–18,360, doi:10.1029/96JC00045.

Michel, C., R. G. Ingram, and L. R. Harris (2006), Variability in oceanographic and ecological processes in the Canadian Arctic Archipelago, *Prog. Oceanogr.*, *71*, 379–401, doi:10.1016/j.pocean.2006.09.006.

Nishi, Y., and S. Tabeta (2005), Analysis of the contribution of ice algae to the ice-covered ecosystem in Lake Saroma by means of a coupled ice-ocean ecosystem model, *J. Mar. Syst.*, *55*(3–4), 249–270, doi:10.1016/j.jmarsys.2004.08.002.

Petrova, V. I., G. I. Batova, A. G. Zinchenko, A. V. Kursheva, and E. V. Narkevskiy (2004), The East Siberian Sea: Distribution, sources, and burial of organic carbon, in *The Arctic Ocean Organic Carbon Cycle Present and Past*, edited by R. Stein and R. W. Macdonald, pp. 204–212, Springer, Berlin.

Rózanska, M., M. Gosselin, M. Poulin, J. M. Wiktor, and C. Michel (2009), Influence of environmental factors on the development of bottom ice protist communities during the winter-spring transition, *Mar. Ecol. Prog. Ser.*, *386*, 43–59, doi:10.3354/meps08092.

Sibert, V., B. Zakardjian, F. Saucier, M. Gosselin, M. Starr, and S. Senneville (2010), Spatial and temporal variability of ice algal production in a 3D ice-ocean model of the Hudson Bay, Hudson Strait and Foxe Basin System, *Polar Res.*, *29*, 353–378, doi:10.1111/j.1751-8369.2010.00184.x.

Smith, R. E. H., W. G. Harrison, L. R. Harris, and A. W. Herman (1990), Vertical fine structure of particulate matter and nutrients in sea ice of the high Arctic, *Can. J. Fish. Aquat. Sci.*, *47*, 1348–1355, doi:10.1139/f90-154.

Stroeve, J., M. M. Holland, W. Meier, T. Scambos, and M. Serreze (2007), Arctic sea ice decline: Faster than forecast, *Geophys. Res. Lett.*, *34*, L09501, doi:10.1029/2007GL029703.

Subba Rao, D. V., and T. Platt (1984), Primary productivity of Arctic waters, *Polar Biol.*, *3*, 191–201, doi:10.1007/BF00292623.

Vetrov, A. A., and E. A. Romankevich (2004), *Carbon Cycle in the Russian Arctic Seas*, Springer, Berlin.

Wakatsuchi, M., and N. Ono (1983), Measurements of salinity and volume of brine excluded from growing sea ice, *J. Geophys. Res.*, *88*, 2943–2951, doi:10.1029/JC088iC05p02943.

C. Deal and M. Jin, International Arctic Research Center, University of Alaska Fairbanks, Fairbanks, AK 99775, USA. (deal@iarc.uaf.edu)

S. Elliott, E. Hunke, N. Jeffery, and M. Maltrud, Coupled Ocean Sea Ice Modeling, Los Alamos National Laboratory, Los Alamos, NM 87545, USA.